Lower and upper bounds for the Rayleigh conductivity of a perforated plate

Sophie Laurens, Sébastien Tordeux, Abderrahmane Bendali, M'Barek Fares, P. Robert Kotiuga

Lower and upper bounds for the Rayleigh conductivity of a perforated plate

S. Laurens* S. Tordeux† A. Bendali‡ M. Fares§ P. R. Kotiuga¶

April 10, 2012

Abstract

Lower and upper bounds for the Rayleigh conductivity of a perforation in a thick plate are usually derived from intuitive approximations and by physical reasoning. This paper addresses a mathematical justification of these approaches. As a byproduct of the rigorous handling of these issues, some improvements to previous bounds for axisymmetric holes are given as well as new estimates for inclined perforations. The main techniques are a proper use of the variational principles of Dirichlet and Kelvin in the context of Beppo-Levi spaces. The derivations are validated by numerical experiments in the two-dimensional axisymmetric case and the full three-dimensional one.

1 Introduction

1.1 Effective impedance boundary conditions

The Rayleigh conductivity is a key ingredient in the construction of effective conditions making it possible to easily account for the transmission and the reflection of an acoustic wave by a plate with small perforations in any easy way. This parameter is involved in most of the models governing the interaction of sound with a perforation: the plain acoustic linear system [14, 25], Howe [7, 8, 9], and Melling models [16]. Contrary to the former model that completely neglects the absorption of acoustic energy by the perforation, the two later ones account for it by means of an aeroacoustic effect and a pure viscosity dissipation respectively. However, numerically computing the Rayleigh conductivity is generally a non trivial task. This problem is three dimensional in general. Its numerical solution thus may become rapidly hard to carry out due to the large size of the problem to be solved. Another difficulty is related to the fact that this problem is set on an unbouded domain so that its numerical solution should be tackled either by a boundary element code [23] or by deriving a radiation condition incorporating the behavior of the solution at infinity in an accurate way (see, e.g., [5, 11]).

To overcome these technical difficulties, many authors proposed to approximate the Rayleigh conductivity by close formulas [1, 7, 10, 19], derived either analytically or by intuitive approaches. In these papers, it is hard to distinguish among the approximations which are heuristic and which can be subject of a rigorous approach. On the one hand, the objective of this paper is to provide a rigorous background for the derivation of such approximations. On the other hand, many studies were devoted to the comparison of these models to acoustic experiments [2, 10, 12, 18, 20]. However, due to the various approximations carried out to derive the models, it is almost impossible to distinguish the modeling errors coming from the approximate estimates of the Rayleigh

*Mathematical Institute of Toulouse (UMR-CNRS 5219), 135 avenue de Rangueil, F-31077 Toulouse, France, sophie.laurens@insa-toulouse.fr

†INRIA Bordeaux Sud-Ouest-LMA (UMR-CNRS 5142), avenue de l'Université, F-64013 Pau, France, sebastien.tordeux@inria.fr

‡INSA-Mathematical Institute of Toulouse (UMR-CNRS 5219), 135 avenue de Rangueil, F-31077 Toulouse, France, abderrahmane.bendali@insa-toulouse.fr

§CERFACS - EMA, 42 avenue Gaspar Coriolis, F-31100 Toulouse, France, fares@cerfacs.fr

¶Boston University, Department of Electrical and Computer Engineering, 8 Saint Mary's Street, Boston MA, 02215, USA, prk@bu.edu

conductivity to those induced by the choice of a specific model. Another objective of this paper is to make this point as clear as possible.

1.2 Definition of the Rayleigh conductivity

Let P be a straight plate with a finite thickness $h > 0$ with one perforation Ω as depicted in Figure 1. Thus, the plate coincides with

$$\mathsf{P} = \left\{ \mathbf{x} \in \mathbb{R}^2 \times [s_-, s_+] \text{ and } \mathbf{x} \notin \Omega \right\}, \tag{1}$$

with $s_+ - s_- = h$, $\Omega \subset \mathbb{R}^2 \times [s_-, s_+]$ a simply connected domain and x_3 in $[s_-, s_+]$. The domain filled by the fluid is $\mathsf{D} = \mathbb{R}^3 \backslash \mathsf{P}$, and can hence be seen as the domain admitting as a non overlapping decomposition Ω and the following two half-spaces

$$\mathsf{D}_+ = \{ \mathbf{x} \in \mathsf{D} \mid x_3 > s_+ \} \text{ and } \mathsf{D}_- = \{ \mathbf{x} \in \mathsf{D} \mid x_3 < s_- \}. \tag{2}$$

We denote by Γ_+ and Γ_- the lower and upper apertures of the perforation Ω, i.e.,

$$\Gamma_\pm \ = \ \{ \mathbf{x} \in \partial\Omega \mid x_3 = s_\pm \}.$$

The lateral part of the boundary of Ω is $\Sigma = \overline{\Omega} \cap \overline{\mathsf{P}}$, hence $\partial\Omega$ can be expressed also in terms of its non overlapping decomposition in Γ_-, Γ_+ and Σ.

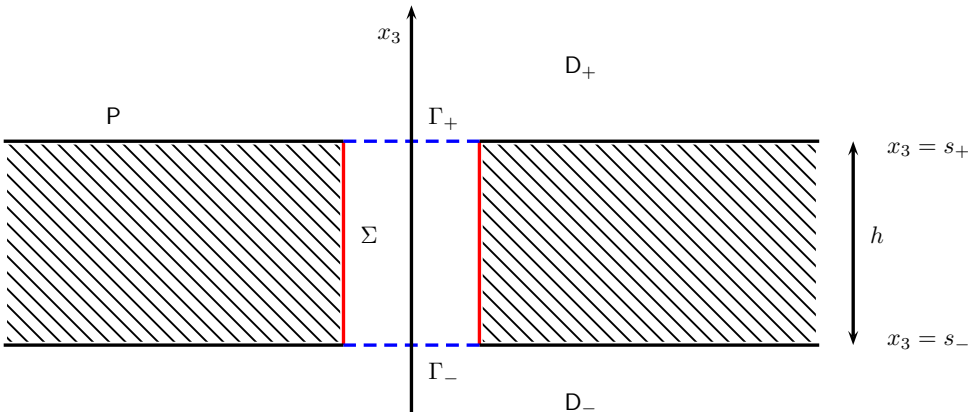

Figure 1: Schematic representation of the domains

The Rayleigh conductivity K_R relates the pressure differentiel from one to the other side of the perforation to the volume flux $Q = \displaystyle\int_{\Gamma_-} v_3 ds = \int_{\Gamma_+} v_3 ds$ through the aperture

$$K_R = \frac{\rho_0 \, \partial_t Q}{P^- - P^+}, \tag{3}$$

with ρ_0 the density of the fluid at rest, v_3 the component along x_3-axis of the velocity $\mathbf{v}$, P^+ and P^- the pressures on the upper and lower side of the perforated plate. The Rayleigh conductivity has the dimension of length, and Eq. (3) is the analogue of Ohm's law.

In several models (cf., e.g., [8, 9, 15, 17]), the Rayleigh conductivity is used as an effective length

$$l = \frac{A}{K_R},$$

where A is the area of the aperture, which expresses the part of the acoustic impedance in the inertial effect of the fluid. The governing equations yielding the Rayleigh conductivity can be expressed in terms of the following boundary-value problem set in the unbounded domain D (cf. [9]):

$$\begin{cases} \rho_0 \partial_t \mathbf{v} + \nabla p = 0, & \text{in } \mathsf{D}, \\ \nabla \cdot \mathbf{v} = 0, & \text{in } \mathsf{D}, \\ \partial_n p = 0, & \text{on } \partial\mathsf{P}, \\ \lim\limits_{|\mathbf{x}|\to+\infty} p(\mathbf{x}) = P^{\pm}, \end{cases} \tag{4}$$

so that

$$K_R = \frac{1}{P^+ - P^-} \int_{\Gamma_+} \partial_3 p(\mathbf{x})\, ds_{\mathbf{x}}. \tag{5}$$

To compute K_R, we introduce the change of unknowns $u = \left(p - \left(P^+ + P^-\right)/2\right) / \left(P^+ - P^-\right)$ that yields the following expression for K_R

$$K_R = \int_{\Gamma_+} \partial_{x_3} u \, ds. \tag{6}$$

Another feature of this change of unknown is that the time derivative in problem (4) can be removed leading to:

$$\begin{cases} \Delta u(\mathbf{x}) = 0 & \text{in } \mathsf{D}, \\ \partial_n u(\mathbf{x}) = 0 & \text{on } \partial\mathsf{P}, \\ \lim\limits_{|x|\to+\infty} u(\mathbf{x}) = \pm 1/2 & \text{on } \mathsf{D}_{\pm}. \end{cases} \tag{7}$$

1.3 Contents of the paper

The present paper is organized as follows. In section 2, some links between Beppo Levi function spaces and the space of functions with square integrable gradients are brought out and made clearer. In section 3, we introduce the Dirichlet and Kelvin dual principles which are the main ingredients for deriving bounds of the Rayleigh conductivity. Section 4 is devoted to the derivation of closed analytical expressions for the bounds for cylindrical, conical and inclined apertures. In Section 5, the obtained formulas are illustrated by numerical experiments. The computations are carried out for the two-dimensional case for an axi-symmetric perforation and with the full three-dimensional library CESC of CERFACS for a general shape.

2 Functions with square integrable gradient

The classical functional setting for solving Laplace problems posed on three-dimensional unbounded domains is the Beppo-Levi space, the space of functions that "weakly tend to zero at infinity" whose gradient is square integrable. Unfortunately, this space is not adapted for the solution of problem (7) whose solution has to be sought in

$$\mathsf{H}(\mathsf{D}) \;=\; \Big\{ v \in H^1_{\rm loc}(\overline{\mathsf{D}}) \mid \nabla v \in L^2(\mathsf{D}) \Big\},$$

where $H^1_{\rm loc}(\overline{\mathsf{D}})$ is the space of functions v defined almost everywhere in D such as $\varphi\, v \in H^1(\mathsf{D})$ for all $\varphi \in \mathcal{D}(\mathbb{R}^3)$. In this section, we clarify the relation between H and the Beppo-Levi space in dimension 3. To prove that problem (7) is well-posed, we first derive a Green formula involving elements in H and vector fields in

$$\mathsf{W}(\mathsf{D}) \;=\; \Big\{ \mathbf{q} \in \mathbf{L}^2(\mathsf{D}) \mid \mathbf{div}\, \mathbf{q} = 0 \text{ in } \mathsf{D} \text{ and } \mathbf{q}\cdot\mathbf{n} = 0 \text{ on } \partial\mathsf{D} \Big\}. \tag{8}$$

Domain A refers either D, D_- or to D_+. The Beppo-Levi space $\mathsf{BL}(\mathsf{A})$ is defined as the closure of $\mathcal{D}(\overline{\mathsf{A}}) = \{u|_{\mathsf{A}} \mid u \in \mathcal{D}(\mathbb{R}^3)\}$ with respect to the H^1 semi-norm

$$|v|_{\mathsf{BL}(\mathsf{A})} = \left(\int_{\mathsf{A}} |\nabla v(\mathbf{x})|^2 \, d\mathbf{x}\right)^{\frac{1}{2}}.$$

It is shown in [6] that $\mathsf{BL}(\mathsf{A})$ can be characterized as a Hilbert space and coincides with the weighted Sobolev space

$$\mathsf{BL}(\mathsf{A}) = \left\{v \in H^1_{\rm loc}(\mathsf{A}) \mid \nabla v \in L^2(\mathsf{A}) \text{ and } \frac{v}{(1+|\mathbf{x}|^2)^{\frac{1}{2}}} \in L^2(\mathsf{A})\right\}. \tag{9}$$

The following proposition collects some usefull properties of functions with square integrable gradients.

Proposition 2.1. *Let $v \in \mathsf{H}$.*

(i) The mean values of v respectively on the hemisphere $\Gamma^R_+ = \{\mathbf{x} \in \mathbb{R}^3 \mid x_3 > s_+ \text{ and } |\mathbf{x} - \mathbf{c}_+| = R\}$ and $\Gamma^R_- = \{\mathbf{x} \in \mathbb{R}^3 \mid x_3 < s_- \text{ and } |\mathbf{x} - \mathbf{c}_-| = R\}$, with $\mathbf{c}_\pm = (0, 0, s_\pm)$, converge as $R \to +\infty$, i.e.,

$$v_\pm := \lim_{R \to +\infty} \frac{1}{2\pi R^2} \int_{\Gamma^R_\pm} v(\mathbf{x}) ds_{\mathbf{x}}.$$

(ii) The restrictions of v to D_- and D_+ satisfy $v|_{\mathsf{D}_\pm} - v_\pm \in \mathsf{BL}(\mathsf{D}_\pm)$.

(iii) The usual Beppo-Levi space $\mathsf{BL}(\mathsf{D})$ can be characterized as $\mathsf{BL}(\mathsf{D}) = \left\{v \in \mathsf{H} \mid v_- = 0 \text{ and } v_+ = 0\right\}$.

(iv) The space H is a Hilbert space when equipped with the inner product

$$(u, v)_{\mathsf{H}} = \int_{\mathsf{D}} \nabla u(\mathbf{x}) \cdot \nabla v(\mathbf{x}) d\mathbf{x} + u_+ \, v_+ + u_- \, v_-. \tag{10}$$

Proof. To prove point (i), we start by denoting $(r_+, \theta_+, \varphi_+)$ the spherical coordinates with origin at $\mathbf{s}_+ = (0, 0, s_+)$

$$x_1 = r_+ \sin\theta_+ \cos\varphi_+, \quad x_2 = r_+ \sin\theta_+ \sin\varphi_+ \quad \text{and} \quad x_3 = s_+ + r_+ \cos\theta_+,$$

and the associated metrics

$$d\sigma_{\mathbf{x}} = \sin\theta_+ \, d\theta_+ d\varphi_+ \quad \text{and} \quad dv_{\mathbf{x}} = \sin\theta_+ \, d\theta_+ d\varphi_+ dr_+.$$

We denote by $\overline{v}(R)$ the mean value of v over the half-sphere Γ^R_+

$$\overline{v}(R) = \frac{1}{2\pi} \int_{\Gamma^R_+} v(\mathbf{x}) d\sigma_{\mathbf{x}} = \frac{1}{2\pi} \int_0^{\pi/2} \int_0^{2\pi} v\,(R, \theta_+, \varphi_+) \, \sin\theta_+ \, d\theta_+ d\varphi_+. \tag{11}$$

Let us prove that $\overline{v}(R)$ satisfies the Cauchy criterion for convergence as R tends to infinity. We have

$$\left|\overline{v}(R') - \overline{v}(R)\right| = \frac{1}{2\pi} \left| \int_{\Gamma^R_+} \Big(v\,(R') - v\,(R)\Big) d\sigma_{\mathbf{x}} \right| \leq \frac{1}{2\pi} \left| \int_{\Gamma^R_+ \times [R, R']} \partial_{r_+} v\,(r_+, \theta_+, \varphi_+) \, dv_{\mathbf{x}} \right|.$$

Applying the Cauchy-Schwartz inequality, we get

$$|\overline{v}(R') - \overline{v}(R)| \leq \frac{1}{2\pi} \left(\int_{\Gamma^R_+ \times [R, R']} \left|\partial_{r_+} v\,(r_+, \theta_+, \varphi_+)\right|^2 \, r_+^2 dv_{\mathbf{x}} \right)^{1/2} \left(\int_{\Gamma^R_+ \times [R, R']} \frac{1}{r_+^2} \, dv_{\mathbf{x}} \right)^{1/2}.$$

This hence establishes the existence of v_+ since

$$|\overline{v}(R') - \overline{v}(R)| \leq \frac{1}{\sqrt{2\pi}} |\nabla v|_{L^2(\mathsf{D}_+)} \left| \frac{1}{R} - \frac{1}{R'} \right| \underset{R, R' \to +\infty}{\longrightarrow} 0. \tag{12}$$

The convergence to v_- is obtained in exactly the same way.

Now, we carry out the proof of point (ii). In view of definition (9) of $\mathsf{BL}(\mathsf{D}_+)$, it is sufficient to show that $\left(v|_{\mathsf{D}_+} - v_+\right) \,/\, \sqrt{1+r_+^2} \in L^2(\mathsf{D}_+)$ or equivalently $\left(v|_{\mathsf{D}_+} - v_+\right) \,/\, \sqrt{1+r_+^2} \in L^2(\mathsf{D}_{+,1})$ with

$$\mathsf{D}_{+,1} = \Big\{ \mathbf{x} \in \mathsf{D}_+ \mid r_+ > 1 \Big\}.$$

This amounts to prove that $\left(v|_{\mathsf{D}_+}(\mathbf{x}) - \overline{v}(r_+)\right) \,/\, \sqrt{1+r_+^2} \in L^2(\mathsf{D}_{+,1})$ and $\left(\overline{v}(r_+) - v_+\right) \,/\, \sqrt{1+r_+^2} \in L^2(\mathsf{D}_{+,1})$. To prove that $\left(v|_{\mathsf{D}_+} - \overline{v}(r_+)\right) \,/\, \sqrt{1+r_+^2} \in L^2(\mathsf{D}_{+,1})$, we observe that

$$\left| \frac{v|_{\mathsf{D}_+} - \overline{v}(r_+)}{(1+r_+^2)^{\frac{1}{2}}} \right|^2_{L^2(\mathsf{D}_{+,1})} = \int_{\mathsf{S}_+} \frac{\Big(v|_{\mathsf{D}_+} - \overline{v}(r_+)\Big)^2}{1+r_+^2} r_+^2 \, dv_{\mathbf{x}} \leq \int_{\mathsf{S}_+} \Big(v\left(r_+, \theta_+, \varphi_+\right) - \overline{v}(r_+)\Big)^2 \, dv_{\mathbf{x}},$$

with S_+ the part of the unit sphere S such that $x_3 > 0$. Using Poincare inequality on the unit sphere, we get

$$\left| \frac{v|_{\mathsf{D}_+} - \overline{v}(r_+)}{(1+r_+^2)^{\frac{1}{2}}} \right|^2_{L^2(\mathsf{D}_{+,1})} \leq C \int_{\mathsf{S}_+} \left(\left(\partial_{\theta_+} v\right)^2 + \left(\frac{\partial_{\varphi_+} v}{\sin\theta_+} \right)^2 \right) dv_{\mathbf{x}}.$$

Since $|\nabla v|^2 = (\partial_{r_+} v)^2 + \left(\frac{1}{r_+} \partial_{\theta_+} v \right)^2 + \left(\frac{1}{r_+ \sin\theta_+} \partial_{\varphi_+} v \right)^2$, we obtain

$$\left| \frac{v|_{\mathsf{D}_+} - \overline{v}(r_+)}{(1+r_+^2)^{\frac{1}{2}}} \right|^2_{L^2(\mathsf{S}_+)} \leq C \int_{\mathsf{S}_+} |\nabla v|^2 \, r_+^2 \, dv_{\mathbf{x}} \leq C |\nabla v|^2_{L^2(\mathsf{S}_+)} < +\infty.$$

Then, we seek to prove that $\left(\overline{v}(r_+) - v_+\right) \,/\, \sqrt{1+r_+^2} \in L^2(\mathsf{S}_+)$. Since

$$\left| \frac{\overline{v}(r_+) - v_+}{(1+r_+^2)^{\frac{1}{2}}} \right|^2_{L^2(\mathsf{D}_{+,1})} = \int_{\mathsf{S}_+} \frac{\left(\overline{v}(r_+) - v_+\right)^2}{1+r_+^2} r_+^2 \, dv_{\mathbf{x}},$$

taking $R = r_+$ and letting R' tend to infinity in Eq. (12), we get

$$|\overline{v}(r_+) - v_+| \leq \frac{1}{\sqrt{2\pi}} |\nabla v|_{L^2(\mathsf{D}_+)} \frac{1}{r_+},$$

and thus

$$\left| \frac{\overline{v}(r_+) - v_+}{(1+r_+^2)^{\frac{1}{2}}} \right|^2_{L^2(\mathsf{D}_{+,1})} \leq \frac{1}{2\pi} |\nabla v|^2_{L^2(\mathsf{D}_+)} \int_{\mathsf{S}_+} \frac{1}{1+r_+^2} \, dv_{\mathbf{x}} \leq \frac{1}{8} |\nabla v|^2_{L^2(\mathsf{D}_+)} < +\infty.$$

Similarly, we have $v|_{\mathsf{D}_-} - v_- \in \mathsf{BL}(\mathsf{D}_-)$.

To prove point (iii), we first establish that $\Big\{ v \in \mathsf{H} \mid v_- = 0 \text{ and } v_+ = 0 \Big\} \subset \mathsf{BL}(\mathsf{D})$. Let $v \in \mathsf{H}$ such as $v_- = v_+ = 0$. It follows from (ii) that $v \in \mathsf{BL}(\mathsf{D}_-)$ and $v \in \mathsf{BL}(\mathsf{D}_+)$. Characterization (9) of BL in terms of weighted Sobolev space yields $v \in \mathsf{BL}(\mathsf{D})$.

Conversely, we prove that $\mathsf{BL}(\mathsf{D}) \subset \Big\{ v \in \mathsf{H} \mid v_- = 0 \text{ and } v_+ = 0 \Big\}$. If $u \in \mathsf{BL}(\mathsf{D})$, it follows from (ii) that $u - u_+ \in \mathsf{BL}(\mathsf{D}_+)$ and that $u - u_- \in \mathsf{BL}(\mathsf{D}_-)$. Therefore, $u_\pm$ belongs to $\mathsf{BL}(\mathsf{D}_\pm)$. This is impossible except if

$u_\pm = 0$ since $\displaystyle\int_{\mathsf{D}_\pm} 1 \,/\, \big(1+|x|^2\big)\; d\mathbf{x} = +\infty$.

This brings us to point (iv). Clearly, $(u,v) \mapsto (u,v)_{\mathsf{H}}$ is a scalar product on H. It first remains to establish that it is an Hilbert space. Let (v_n) be a Cauchy sequence in H. Denoting by $\xi_\pm$ two cut-off functions such as $\xi_\pm(\mathbf{x}) = 1$ in $\mathsf{D}_\pm$ and $\xi_\pm(\mathbf{x}) = 0$ in $\mathsf{D}_\mp$, we consider the function

$$w_n = v_n - (v_n)_+\xi_+ - (v_n)_-\xi_-,$$

that belongs to $\mathsf{BL}(\mathsf{D})$ as established in (ii). We first remark that (w_n) is a Cauchy sequence of $\mathsf{BL}(\mathsf{D})$ equipped with its natural norm $|v|_{\mathsf{BL}(\mathsf{D})} = |\nabla v|_{L^2(\mathsf{D})}$ since ∇v_n is a Cauchy sequence in $L^2(\mathsf{D})$ and $(v_n)_+$, $(v_n)_-$ are convergent

$$(v_n)_+ \longrightarrow \overline{v}_+ \quad \text{and} \quad (v_n)_- \longrightarrow \overline{v}_- \quad \text{with } v_+,\ v_- \in \mathbb{R}. \tag{13}$$

It follows from the completeness of $\mathsf{BL}(\mathsf{D})$ that w_n converges to $w \in \mathsf{BL}(\mathsf{D})$

$$\nabla w_n \longrightarrow \nabla w \quad \text{in } L^2(\mathsf{D}).$$

The function $v = w + \xi_+\overline{v}_+ + \xi_-\overline{v}_-$ belongs to H and satisfies $v_+ = \overline{v}_+$, $v_- = \overline{v}_-$. To complete the proof, it just remains to establish that v_n converges to v in H

$$\left\{\begin{array}{ll} |\nabla(v_n - v)|_{L^2(\mathsf{D})} & \leq |\nabla(w_n - w) + \big((v_n)_+ - \overline{v}_+\big)\xi_+ + \big((v_n)_- - \overline{v}_-\big)\xi_-|_{L^2(\mathsf{D})} \\ & \leq |\nabla(w_n - w)| + |\big((v_n)_+ - \overline{v}_+\big)\xi_+| + |\big((v_n)_- - \overline{v}_-\big)\xi_-| \underset{n\to+\infty}{\to} 0. \\ |(v_n)_\pm - v_\pm| & = |(v_n)_\pm - \overline{v}_\pm| \to 0 \text{ when } n \to \pm\infty. \end{array}\right. \tag{14}$$

The following lemma establishes the above mentioned Green's formula involving a function v in H and a scalar field $\mathbf{q}$ in W.

Lemma 2.1. *For all $v \in \mathsf{H}$ and $q \in \mathsf{W}$, the following Green's formula holds true*

$$\int_{\mathsf{D}} \nabla v(\mathbf{x}) \cdot \mathbf{q}(\mathbf{x}) d\mathbf{x} \;= (v_+ - v_-) \int_{\Gamma_\pm} q_3(\mathbf{x})\; ds_{\mathbf{x}}.$$

Proof. Let $\mathsf{A} = \mathsf{D}$, D_+ or D_-. For $w \in \mathsf{BL}(\mathsf{A})$ and $\mathbf{q} \in \mathsf{W}$ defined in Eq. (8), Green's formula yields ([6])

$$\int_{\mathsf{A}} \nabla w(\mathbf{x}) \cdot \mathbf{q}(\mathbf{x}) d\mathbf{x} = \int_{\partial\mathsf{A}} w(\mathbf{x})\; \mathbf{q}(\mathbf{x}) \cdot \mathbf{n}\; ds_{\mathbf{x}},$$

where $ds_{\mathbf{x}}$ is the elemental area on $\partial\mathsf{A}$. The integral $I = \displaystyle\int_{\mathsf{D}} \nabla v(\mathbf{x}) \cdot \mathbf{q}(\mathbf{x}) d\mathbf{x}$ is decomposed into three parts which are separately expressed by means of a Green's formula because $v|_{\mathsf{D}_\pm} - v_\pm \in \mathsf{BL}(\mathsf{D}_\pm)$.

$$\left\{\begin{array}{l} \displaystyle\int_{\mathsf{D}_\pm} \nabla v(\mathbf{x}) \cdot \mathbf{q}(\mathbf{x}) d\mathbf{x} = \int_{\mathsf{D}_\pm} \nabla\Big(v(\mathbf{x}) - v_\pm\Big) \cdot \mathbf{q}(\mathbf{x}) d\mathbf{x} \;=\; \mp \int_{\Gamma_\pm} \Big(v(\mathbf{x}) - v_\pm\Big) q_3(\mathbf{x}) ds_{\mathbf{x}}, \\ \displaystyle\int_{\Omega} \nabla v(\mathbf{x}) \cdot \mathbf{q}(\mathbf{x}) d\mathbf{x} = \int_{\Gamma_+} v(\mathbf{x}) q_3(\mathbf{x}) ds_{\mathbf{x}} - \int_{\Gamma_-} v(\mathbf{x}) q_3(\mathbf{x}) ds_{\mathbf{x}}. \end{array}\right. \tag{15}$$

Since $\displaystyle\int_{\Gamma_-} q_3(\mathbf{x})\; ds_{\mathbf{x}} = \int_{\Gamma_+} q_3(\mathbf{x})\; ds_{\mathbf{x}}$, we sum the above conditions to obtain $I = (v_+ - v_-) \displaystyle\int_{\Gamma_-} q_3(\mathbf{x})\; ds_{\mathbf{x}}$.

Lemma 2.2. *There exists a unique solution $u \in \mathsf{H}$ to problem (7) characterized by $u \in \mathsf{H}_{1/2}$ and $\nabla u \in \mathsf{W}$, where $\mathsf{H}_{1/2}$ is the affine space*

$$\mathsf{H}_{1/2} \;=\; \Big\{v \in \mathsf{H} \mid v_+ = 1/2 \text{ and } v_- = -1/2\Big\}.$$

Proof. Let us first recall a similar result in $\mathsf{BL}(\mathsf{D})$ [6]. For $f \in \mathcal{D}(\mathsf{D})$ and $g \in \mathcal{D}(\partial\mathsf{D})$, there exists one and only one $u \in \mathsf{BL}(\mathsf{D})$ such that

$$\Delta u = f \text{ in } \mathsf{D} \quad \text{and} \quad \partial_{\mathbf{n}} u = g \text{ on } \partial\mathsf{D}. \tag{16}$$

We first start establishing the uniqueness of the solution. If $u_1 \in \mathsf{H}$ and $u_2 \in \mathsf{H}$ are two solutions to (7), $w = u_1 - u_2$ belongs to $\mathsf{BL}(\mathsf{D})$ and satisfies $\Delta w = 0$ in D and $\partial_n w = 0$ on $\partial\mathsf{D}$. Property (16) directly yields that $w = 0$.
We now move on to seeking a solution. Let us define $w \in \mathsf{BL}(\mathsf{D})$ by

$$\Delta w = -\frac{\Delta\xi_+}{2} + \frac{\Delta\xi_-}{2} \text{ and } \partial_n w = -\frac{\partial_n\xi_+}{2} + \frac{\partial_n\xi_-}{2}.$$

Function $u = w + \xi_+ \,/\, 2 - \xi_- \,/\, 2 \in \mathsf{H}_{1/2}$ and satisfies

$$\Delta u(\mathbf{x}) = 0 \text{ in } \mathsf{D} \text{ and } \partial_n u(\mathbf{x}) = 0 \text{ on } \partial\mathsf{D}.$$

It remains to prove that $\lim\limits_{|x|\to+\infty} u(\mathbf{x}) = 1/2$ on D_+ and $\lim\limits_{|x|\to+\infty} u(\mathbf{x}) = -1/2$ on D_-. This last point is easily obtained by a separation of variables. ⊠

3 The Dirichlet and Kelvin principles

The Dirichlet and Kelvin principles[1] are two variational principles, dual each to the other. This theory, which takes its roots in Lagrangian and Hamiltonian mechanics, is of great importance in several areas, particularly in mathematical modeling [4, Chap 4, Sect 9] to obtain lower and upper bounds for potential and kinetic energies, in optimization [13] to derive the dual formulations, and in numerical analysis [22, Chap 1] for assessing the validity or the accuracy of a numerical solution.

In this paper, these dual variational principles offer an ad-hoc framework to derive lower and upper bounds of the Rayleigh conductivity K_R.

Proposition 3.1. *The Rayleigh conductivity K_R can be obtained equivalently in one of the following ways:*

$$\begin{cases} \textbf{\textit{Dirichlet principle:}}\ K_R = \min\limits_{v\in\mathsf{H}_{1/2}} \mathsf{J}_1(v) \ \textit{with}\ \mathsf{J}_1(v) = \displaystyle\int_{\mathsf{D}} \left|\nabla v(\mathbf{x})\right|^2 d\mathbf{x} \\ \textbf{\textit{Kelvin principle:}}\ K_R = \max\limits_{\mathbf{q}\in\mathsf{W}} \mathsf{J}_2(\mathbf{q}) \ \textit{with}\ \mathsf{J}_2(\mathbf{q}) = 2\displaystyle\int_{\Gamma_-} q_3(\mathbf{x})\, ds_{\mathbf{x}} - \int_{\mathsf{D}} |\mathbf{q}(\mathbf{x})|^2\, d\mathbf{x}. \end{cases} \tag{17}$$

Proof. Let $\mathsf{J} : \mathsf{H} \times L^2(\mathsf{D}) \longrightarrow \mathbb{R}^+$ be the functional

$$\mathsf{J}(v, \mathbf{q}) = \int_{\mathsf{D}} |\mathbf{q}(\mathbf{x}) - \nabla v(\mathbf{x})|^2 \, d\mathbf{x}.$$

We first prove that $(u, \nabla u)$ is the unique element of $\mathsf{H}_{1/2} \times \mathsf{W}$ where J reachs its minimum. Lemma 2.2 gives that the solution to problem (7) satisfies

$$\mathsf{J}(u, \nabla u) = 0, \quad u \in \mathsf{H}_{1/2}, \quad \nabla u \in \mathsf{W}.$$

Thus $(u, \nabla u)$ is a point where J reaches its minimum on $\mathsf{H}_{1/2} \times \mathsf{W}$. On the other hand, every $(v, \mathbf{q}) \in \mathsf{H}_{1/2} \times \mathsf{W}$ satisfying $\mathsf{J}(v, \mathbf{q}) = 0$ is such that $\nabla v = \mathbf{q}$. Lemma 2.2 directly yields $v = u$ and $\mathbf{q} = \nabla u$. The above claim is thus proved.

[1] In the context of electrostatics, the Kelvin principle is also called the Thompson principle. William Thompson is the name at birth of Lord Kelvin.

We now show that J_1 reachs its minimum at u and J_2 its maximum at ∇u. Lemma (2.1) gives that, for all $v \in \mathsf{H}_{1/2}$ and $\mathbf{q} \in \mathsf{W}$

$$\int_{\mathsf{D}} \nabla v(\mathbf{x}) \cdot \mathbf{q}(\mathbf{x}) d\mathbf{x} \;=\; (v_+ - v_-) \int_{\Gamma_-} q_3(\mathbf{x})\; ds_{\mathbf{x}} \;=\; \int_{\Gamma_-} q_3(\mathbf{x})\; ds_{\mathbf{x}}. \tag{18}$$

It follows that $\mathsf{J}(v, \mathbf{q}) \;=\; \mathsf{J}_1(v) - \mathsf{J}_2(\mathbf{q})$ thus establishing that $\mathsf{J}_1(u) \leq \mathsf{J}_1(v)$ for all $v \in \mathsf{H}_{1/2}$ and $\mathsf{J}_1(\mathbf{q}) \leq \mathsf{J}_1(\nabla u)$ for all $\mathbf{q} \in \mathsf{W}$.

Finally we prove that $K_R = \mathsf{J}_1(u) = \mathsf{J}_2(\nabla u)$. Since $\mathsf{J}(u, \nabla u) = \mathsf{J}_1(u) - \mathsf{J}_2(\nabla u) = 0$, we have $\mathsf{J}_1(u) = \mathsf{J}_2(\nabla u)$. To conclude, it remains to prove that $\mathsf{J}_1(u) = K_R$. Substituting u for v and ∇u for $\mathbf{q}$ in (18), we readily get $\mathsf{J}_1(u) \;=\; \displaystyle\int_{\mathsf{D}} |\nabla u(\mathbf{x})|^2 \; d\mathbf{x} \;=\; \int_{\Gamma_-} \partial_{x_3} u(\mathbf{x})\; ds_{\mathbf{x}} \;=\; K_R.$ ⊠

4 Bounds for the Rayleigh conductivity of some usual perforations

Proposition 3.1 is used to get upper and lower bounds for the Rayleigh conductivity for usual perforations. We consider axi-symmetric geometries, related to cylindrical and conical apertures, as well as perforations which give rise to a full three-dimensional problem.

4.1 Cylindrical apertures

Here, we consider a cylindrical perforation $\Omega = \Big\{(x_1, x_2, x_3) \in \mathbb{R}^3 \mid (x_1, x_2) \in \mathsf{S}_R \text{ and } x_3 \in [s_-, s_+]\Big\}$ with circular section $\mathsf{S}_R = \Big\{(x_1, x_2) \in \mathbb{R}^2 \mid x_1^2 + x_2^2 < R\Big\}$ (see Figure 2 below).

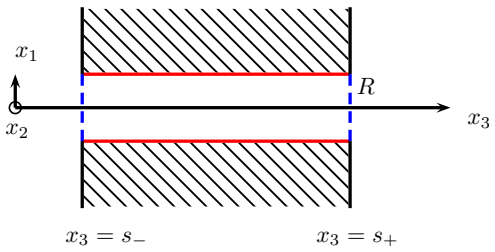

Figure 2: Cylindrical aperture of radius R

Theorem 4.1. *For a cylindrical perforation, we have the following bounds for its Rayleigh conductivity:*

$$K^-_{R,\mathrm{cyl}} \leq K_{R,\mathrm{cyl}} \leq K^+_{R,\mathrm{cyl}} \qquad \textit{with } K^-_{R,\mathrm{cyl}} \;=\; \frac{\pi R^2}{h + 16R\,/\,3\pi} \textit{ and } K^+_{R,\mathrm{cyl}} \;=\; \frac{\pi R^2}{h + \pi R/2}. \tag{19}$$

Proof. As established above, the Dirichlet principle allows us to obtain the upper bound

$$K_{R,\mathrm{cyl}} \leq \mathsf{J}_1(v) \text{ for all } v \in \mathsf{H}_{1/2}. \tag{20}$$

We first consider the following problem

$$\begin{cases} \Delta w_R(\mathbf{x}) = 0 & \text{for } x_3 \neq 0, \\ \partial_{x_3} w_R(x_1, x_2, 0) = 0 & \text{for } x_1^2 + x_2^2 > R^2, \\ w_R(x_1, x_2, 0) = 1/2 & \text{for } x_1^2 + x_2^2 < R^2, \end{cases} \tag{21}$$

whose solution $w_R \in \mathsf{BL}(\mathbb{R}^3)$ can be expressed analytically by ([24, §3.4, pp 72])

$$w_R(\mathbf{x}) = \frac{1}{2\pi^2} \int_{\mathsf{B}_R} \frac{1}{\sqrt{R^2 - |\mathbf{y}|^2}} \frac{ds_{\mathbf{y}}}{|\mathbf{x}-\mathbf{y}|} \quad \text{for } x_3 \neq 0, \tag{22}$$

with $\mathsf{B}_R = \{(y_1, y_2, y_3) \in \mathbb{R}^3 \mid y_1^2 + y_2^2 < R^2 \text{ and } y_3 = 0\}$. For $\alpha = (\alpha_+, \alpha_-) \in \mathbb{R}^2$ a pair of real numbers, we denote by $v_\alpha : \mathsf{D} \longrightarrow \mathbb{C}$ the function defined by

$$v_\alpha(\mathbf{x}) = \begin{cases} 1/2 - (1-2\alpha_+)\, w_R(x_1, x_2, x_3 - s_+) & \text{for } x_3 > s_+, \\ \alpha_- + (\alpha_+ - \alpha_-)\,(x_3 - s_-)\,/\,h & \text{for } s_- < x_3 < s_+, \\ -1/2 + (1+2\alpha_-)\, w_R(x_1, x_2, x_3 - s_-) & \text{for } x_3 < s_-. \end{cases}$$

Proposition 2.1 gives that $v_\alpha \in \mathsf{H}_{1/2}$. Lemma A.1 in Appendix A then yields

$$\int_{\mathsf{D}_\pm} |\nabla w_R(x_1, x_2, x_3 - s_\pm)|^2 d\mathbf{x} = R.$$

Hence,

$$\begin{aligned} \mathsf{J}_1(v_\alpha) &= \int_{\mathsf{D}} |\nabla v_\alpha(\mathbf{x})|^2 \, d\mathbf{x} = \int_{\mathsf{D}_+} |\nabla v_\alpha(\mathbf{x})|^2 \, d\mathbf{x} + \int_{\Omega} |\nabla v_\alpha(\mathbf{x})|^2 \, d\mathbf{x} + \int_{\mathsf{D}_-} |\nabla v_\alpha(\mathbf{x})|^2 \, d\mathbf{x} \\ &= R\big(1-2\alpha_+\big)^2 + (\alpha_+ - \alpha_-)^2 \, \pi R^2/h + R\,(1+2\alpha_-)^2 \,. \end{aligned} \tag{23}$$

Solving this elementary minimization problem, we get $\alpha_- = \alpha_+ = h/\,(\pi R + 2h)$ and $\mathsf{J}_1(v_\alpha) = \pi R^2\,/\,(h + \pi R/2)$.

The lower bound is obtained from the Kelvin principle

$$K_{R,\mathrm{cyl}} \geq \mathsf{J}_2(\mathbf{q}) \text{ for all } \mathbf{q} \text{ in } \mathsf{W}. \tag{24}$$

We consider the problem

$$\begin{cases} \Delta z_R(\mathbf{x}) = 0 & \text{for } x_3 \neq 0, \\ \partial_{x_3} z_R(x_1, x_2, 0) = 0 & \text{for } x_1^2 + x_2^2 > R^2, \\ \partial_{x_3} z_R(x_1, x_2, 0_\pm) = \pm 1/2 & \text{for } x_1^2 + x_2^2 < R^2, \end{cases} \tag{25}$$

whose solution $z_R \in \mathsf{BL}(\mathbb{R}^3)$ can be expressed in terms of the following integral [23]

$$z_R(\mathbf{x}) = \frac{1}{2\pi} \int_{\mathsf{B}_R} \frac{1}{|\mathbf{x}-\mathbf{y}|} ds_{\mathbf{y}} \quad \text{for } x_3 \neq 0. \tag{26}$$

This defines $\mathbf{q}_\beta \in \mathsf{W}$, up to a multiplicative constant $\beta \in \mathbb{R}$, such that

$$\mathbf{q}_\beta(\mathbf{x}) = \begin{cases} \beta\, \nabla z_R(x_1, x_2, x_3 - s_+)\,/\,\pi R^2 & \text{for } x_3 > s_+, \\ \beta\, \mathbf{e}_3\,/\,\pi R^2 & \text{for } s_- < x_3 < s_+, \\ -\beta\, \nabla z_R(x_1, x_2, x_3 - s_-)\,/\,\pi R^2 & \text{for } x_3 < s_-. \end{cases}$$

Using the non overlapping decomposition of D in D_+, D_- and Ω, we can express $\mathsf{J}_2(\mathbf{q}_\beta)$ as follows

$$\begin{aligned} \mathsf{J}_2(\mathbf{q}_\beta) &= 2\int_{\Gamma_-} \mathbf{q}_\beta(\mathbf{x}) \cdot \mathbf{e}_3 ds_{\mathbf{x}} - \int_{\mathsf{D}} |\mathbf{q}_\beta|^2 d\mathbf{x} = 2\beta - \Big(\int_{\mathsf{D}_+} |\mathbf{q}_\beta|^2 d\mathbf{x} + \int_{\mathsf{D}_-} |\mathbf{q}_\beta|^2 d\mathbf{x} + \int_{\Omega} |\mathbf{q}_\beta|^2 d\mathbf{x} \Big) \\ &= 2\beta - \frac{\beta^2}{\pi^2\, R^4} \left(\int_{x_3>0} |\nabla z_R|^2 d\mathbf{x} + \int_{x_3<0} |\nabla z_R|^2 d\mathbf{x} + \pi R^2 h \right) = 2\beta - \left(\frac{16R}{3\pi} + h \right) \frac{\beta^2}{\pi R^2}. \end{aligned}$$

Integral $\displaystyle\int_{\pm x_3>0} \left|\nabla z_R(\mathbf{x})\right|^2 d\mathbf{x} = 8R^3/3$ is calculated in Appendix A (Lemma A.1). Maximizing this expression in β, we obtain $\beta = \dfrac{\pi R^2}{h + 16R/3\pi}$, hence $\mathsf{J}_2(\mathbf{q}_\beta) = \dfrac{\pi R^2}{h + 16R/3\pi}$. ⊠

Remark 4.1. *Estimate* (19) *was stated by Rayleigh [21], then Howe [9, section 5.3] and mostly obtained by physical reasoning. Here, the actual new feature of this approach is to rely on rigorous arguments only.*

4.2 Conical apertures

We consider now a conical aperture of the following form

$$\Omega = \left\{\mathbf{x} \in \mathbb{R}^3 \mid (x_1, x_2) \in \mathsf{S}_{R(x_3)} \text{ and } x_3 \in [s_-, s_+]\right\}$$

where the radius $R(s)$ is linearly varying from R_- to R_+(see Figure 3 below)

$$R(s) = R_- + \frac{s - s_-}{h}(R_+ - R_-) = R_- + (s - s_-)\,\tan\varphi \quad \text{with } R_+ > R_-. \tag{27}$$

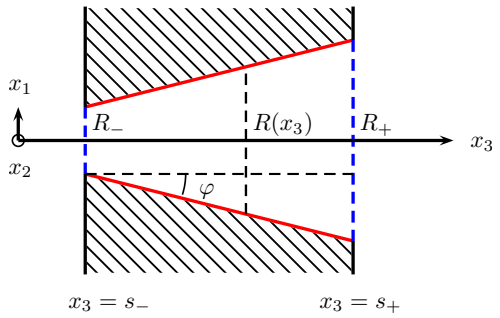

Figure 3: Conical aperture of radius $R(x_3)$.

Theorem 4.2. *The following bounds of a conical aperture holds true*

$$K^-_{R,\mathrm{con}} \le K_{R,\mathrm{con}} \le K^+_{R,\mathrm{con}}, \tag{28}$$

with

$$K^-_{R,\mathrm{con}} = \frac{\pi R_- R_+}{h + \dfrac{8}{3\pi}(R_- + R_+) + \dfrac{1}{2h}(R_- - R_+)^2} \quad \textit{and} \quad K^+_{R,\mathrm{con}} = \frac{\pi R_- R_+}{h + \dfrac{\pi}{4}(R_- + R_+)},$$

or equivalently

$$K^-_{R,\mathrm{con}} = \frac{\pi R_-(R_- + h\,\tan\varphi)}{\dfrac{16R_-}{3\pi} + h\Big(1 + \dfrac{8}{3\pi}\,\tan\varphi + \dfrac{1}{2}\,\tan^2\varphi\Big)} \quad \textit{and} \quad K^+_{R,\mathrm{con}} = \frac{\pi R_-(R_- + h\,\tan\varphi)}{\dfrac{\pi R_-}{2} + h\Big(1 + \dfrac{\pi}{4}\,\tan\varphi\Big)}.$$

Proof. We follow the same approach as in theorem 4.1.
To establish the upper bound, we consider $v_\alpha \in \mathsf{H}_{1/2}$ depending on two real constants α_- and α_+:

$$v_\alpha(\mathbf{x}) = \begin{cases} 1/2 - (1 - 2\alpha_+)\, w_{R_+}(x_1, x_2, x_3 - s_+) & \text{for } x_3 > s_+, \\ \alpha_- + \Big(\alpha_+ - \alpha_-\Big) \dfrac{\displaystyle\int_{s_-}^{x_3} \frac{dx_3}{\pi R^2(x_3)}}{\displaystyle\int_{s_-}^{s_+} \frac{dx_3}{\pi R^2(x_3)}} & \text{for } s_- < x_3 < s_+, \\ -1/2 + (1 + 2\alpha_-)\, w_{R_-}(x_1, x_2, x_3 - s_-) & \text{for } x_3 < s_-, \end{cases}$$

where $w_{R_\pm}$ is the function w_R defined in (21) with $R = R_\pm$. Similarily as in the proof of theorem 4.1, we get

$$\begin{aligned}\mathsf{J}_1(v_\alpha) &= \int_{\mathsf{D}_+\cup\mathsf{D}_-} |\nabla v_\alpha(\mathbf{x})|^2\, d\mathbf{x} + \int_\Omega |\nabla v_\alpha(\mathbf{x})|^2\, d\mathbf{x} \\ &= R_-\,(1+2\alpha_-)^2 + R_+\,(1-2\alpha_+)^2 + (\alpha_+-\alpha_-)^2\,\pi R_+R_-/h.\end{aligned}$$

As above, we minimize $\mathsf{J}_1(v_\alpha)$ in α to get

$$\alpha_\pm = \pm\frac{1}{2} \mp \frac{R_\mp \pi}{\pi(R_+ + R_-) + 4h} \quad \text{and so} \quad \mathsf{J}_1(v_\alpha) = \frac{4\pi R_+R_-}{\pi(R_+ + R_-) + 4h}.$$

To obtain the lower bound, we consider the vector field $\mathbf{q}_\beta \in \mathsf{W}$, with $\beta \in \mathbb{R}$, given by

$$\mathbf{q}_\beta(\mathbf{x}) = \begin{cases} \dfrac{\beta}{\pi\, R_+^2}\, \nabla z_{R_+}(x_1, x_2, x_3 - s_+) & \text{for } x_3 > s_+, \\ \dfrac{\beta}{\pi\, R^2(x_3)} \left(\mathbf{e}_3 + \dfrac{r}{R(x_3)} \dfrac{R_+ - R_-}{h} \mathbf{e}_r\right) & \text{for } s_- < x_3 < s_+, \\ -\dfrac{\beta}{\pi\, R_-^2}\, \nabla z_{R_-}(x_1, x_2, x_3 - s_-) & \text{for } x_3 < s_-, \end{cases}$$

with z_R the function defined in (25). Proceeding as in the proof of theorem 4.1, we get

$$\begin{aligned}\mathsf{J}_2(\mathbf{q}_\beta) &= 2\int_{\Gamma_-} \mathbf{q}_\beta(\mathbf{x})\cdot\mathbf{e}_3 ds_{\mathbf{x}} - \Big(\int_{\mathsf{D}_+} |\mathbf{q}_\beta|^2 d\mathbf{x} + \int_{\mathsf{D}_-} |\mathbf{q}_\beta|^2 d\mathbf{x} + \int_\Omega |\mathbf{q}_\beta|^2 d\mathbf{x}\Big) \\ &= 2\beta - \frac{\beta^2}{\pi^2\, R_\pm^4} \int_\Omega |\nabla z_{R_\pm}|^2 d\mathbf{x} + \frac{\beta^2}{\pi^2} \int_\Omega \left(1 + \frac{r^2}{R^2(x_3)} \left(\frac{R_+ - R_-}{h}\right)^2\right) \frac{dx_3}{R^4(x_3)} \\ &= 2\beta - \beta^2 \left(\frac{8}{3\pi^2}\, \frac{R_+ + R_-}{R_+R_-} + \frac{h}{\pi R_- R_+} \left(1 + \frac{1}{2}\left(\frac{R_+ - R_-}{h}\right)^2\right)\right).\end{aligned}$$

It is then easy to maximize $\mathsf{J}_2(\mathbf{q}_\beta)$ in β to get $\mathsf{J}_2(\mathbf{q}_\beta) = \pi R_- R_+ \,/\, \left(h + \frac{8}{3\pi}(R_+ + R_-) + \frac{1}{2h}(R_+ - R_-)^2\right)$. ⊠

Remark 4.2. *Bounds* (28) *of Theorem 4.2 have to be compared with the following estimates obtained by Howe [9, page 359, section* 5.3*]:*

$$\frac{h}{\pi\, R_-\, R_+} + \frac{1}{4}\left(\frac{1}{R_-} + \frac{1}{R_+}\right) \le \frac{1}{K_R} \le \frac{h}{\pi\, R_-\, R_+} + \frac{(R_+ - R_-)^2}{\pi\, R_-\, R_+\, h} + \frac{8}{3\pi^2}\left(\frac{1}{R_-} + \frac{1}{R_+}\right).$$

Putting them in the same form as (28)*, we get*

$$K^-_{R,\mathrm{Howe}} = \frac{\pi R_- R_+}{h + \dfrac{8}{3\pi}(R_- + R_+) + \dfrac{1}{h}(R_- - R_+)^2} \quad \textit{and} \quad K^+_{R,\mathrm{Howe}} = \frac{\pi R_- R_+}{h + \dfrac{\pi}{4}(R_- + R_+)}.$$

There is a missed factor 2 *in the last term in the denominator of the fraction expressing* $K^-_{R,\mathrm{Howe}}$ *which seems to be a mistyping.*

4.3 Inclined cylinder

We are now investigating the case where the aperture is cylindrical and inclined with an angle θ :

$$\Omega = \Big\{\mathbf{x} \in \mathbb{R}^3 \mid (\widehat{x}_1(\mathbf{x}), x_2) \in \mathsf{S}_R \text{ and } x_3 \in [s_-, s_+] \text{ with } \widehat{x}_1(\mathbf{x}) = x_1 - (x_3 - s_-)\,\tan\theta\Big\}.$$

The perforation was chosen in such a way that its section along the normal to the plate is circular with a radius linearly varying from $R_- = R(s_-)$ to $R_+ = R(s_+)$ (see Figure 4 below).

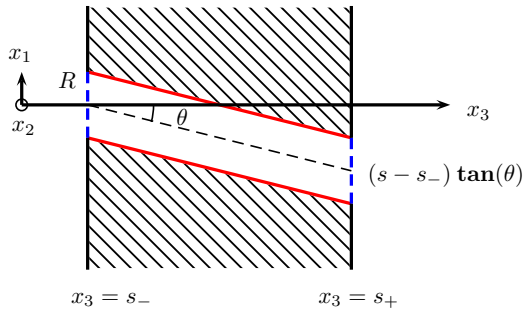

Figure 4: Cylindrical aperture inclined with angle θ with respect to the x_3 axis

Theorem 4.3. *The following bounds hold true for an inclined perforation*

$$K^-_{R,\mathrm{inc}} \le K_{R,\mathrm{inc}} \le K^+_{R,\mathrm{inc}}, \tag{29}$$

with

$$K^-_{R,\mathrm{inc}} = \frac{\pi R^2}{\dfrac{16R}{3\pi} + \dfrac{h}{\cos^2\theta}} \text{ and } K^+_{R,\mathrm{inc}} = \frac{\pi R^2}{\dfrac{\pi R}{2} + \dfrac{h}{\cos^2\theta}\Big(1 + \dfrac{16R}{3\pi h}\sin^2\theta\Big)^{-1}}.$$

Proof. As above, we start with the upper bound. We consider $v_\alpha \in \mathsf{H}_{1/2}$ depending, here too, on two real constants α_- and α_+:

$$v_\alpha(\mathbf{x}) = \begin{cases} 1/2 - (1-2\alpha)\ w_R(\widehat{x}_1, x_2, x_3 - s_+) + \dfrac{\mu_\alpha\ \sin\theta}{h}\, t_R(\widehat{x}_1, x_2, x_3 - s_+) & \text{for } x_3 > s_+, \\ -\alpha + \dfrac{\mu_\alpha}{h}\Big((x_3 - s_-)\ \cos\theta + x_1\ \sin\theta\Big) & \text{for } s_- < x_3 < s_+, \\ -1/2 + (1-2\alpha)\ w_R(\widehat{x}_1, x_2, x_3 - s_-) + \dfrac{\mu_\alpha\ \sin\theta}{h}\, t_R(\widehat{x}_1, x_2, x_3 - s_-) & \text{for } x_3 < s_-, \end{cases}$$

with $\mu_\alpha = 2\alpha\ \cos\theta$, w_R given in (22) and $t_R \in \mathsf{BL}(\mathbb{R}^3)$ defined by

$$\begin{cases} \Delta t_R(\mathbf{x}) = 0, & \text{for } x_3 \neq 0, \\ \partial_{x_3} t_R(x_1, x_2, 0) = 0, & \text{for } x_1^2 + x_2^2 > R^2, \\ t_R(x_1, x_2, 0) = x_1, & \text{for } x_1^2 + x_2^2 < R^2. \end{cases} \tag{30}$$

Using Copson's method [24, §3.4, pp 72], an explicit integral expression can be given for t_R:

$$t_R(\mathbf{x}) = \frac{2}{\pi^2}\int_{\mathsf{S}_R} \frac{y_1}{\sqrt{R^2 - |\mathbf{y}|^2}}\,\frac{ds_{\mathbf{y}}}{|\mathbf{x} - \mathbf{y}|} \quad \text{for } x_3 \neq 0. \tag{31}$$

Making use of the calculations carried out in Appendix A, it follows:

$$\begin{aligned} \mathsf{J}_1(v_\alpha) &= \int_{\mathsf{D}} |\nabla v_\alpha(\mathbf{x})|^2\, d\mathbf{x} = \int_{\mathsf{D}_+} |\nabla v_\alpha(\mathbf{x})|^2\, d\mathbf{x} + \int_{\Omega} |\nabla v_\alpha(\mathbf{x})|^2\, d\mathbf{x} + \int_{\mathsf{D}_-} |\nabla v_\alpha(\mathbf{x})|^2\, d\mathbf{x} \\ &= 2\left(R(1-2\alpha)^2 + \frac{\mu_\alpha^2\ \sin^2\theta}{h^2}\ \frac{8R^3}{3}\right) + \frac{\mu_\alpha^2}{h^2}\,\pi R^2 h. \end{aligned} \tag{32}$$

As above, we maximize $\mathsf{J}_1(v_\alpha)$ in α and obtain $\alpha = 4R/\Big(8R + 4\cos^2\theta/h^2\,\big(16R^3\,\sin^2\theta/3 + \pi R^2 h\big)\Big)$,

$$\mathsf{J}_1(v_\alpha) = \frac{\pi R^2\Big(1 + \dfrac{16R}{3\pi h}\sin^2\theta\Big)}{\dfrac{h}{\cos^2\theta} + \dfrac{\pi R}{2}\Big(1 + \dfrac{16R}{3\pi h}\sin^2\theta\Big)}.$$

We now establish the lower bound. Let us consider the vector field $\mathbf{q}_\beta \in \mathsf{W}$, with $\beta \in \mathbb{R}$, given by

$$\mathbf{q}_\beta(\mathbf{x}) = \begin{cases} \dfrac{\beta}{\pi\, R^2}\,\nabla z_R(\widehat{x}_1, x_2, x_3 - s_+) & \text{for } x_3 > s_+, \\ \dfrac{\beta}{\pi\, R^2}\,\Big(\mathbf{e}_3 + \tan\theta\,\mathbf{e}_1\Big) & \text{for } s_- < x_3 < s_+, \\ -\dfrac{\beta}{\pi\, R^2}\,\nabla z_R(\widehat{x}_1, x_2, x_3 - s_-) & \text{for } x_3 < s_-. \end{cases}$$

with z_R the function defined in (25). We have

$$\mathsf{J}_2(\mathbf{q}_\beta) = 2\int_{\Gamma_-} \mathbf{q}_\beta(\mathbf{x})\cdot\mathbf{e}_3 ds_{\mathbf{x}} - \int_{\mathsf{D}_+\cup\mathsf{D}_-\cup\Omega} |\mathbf{q}_\beta|^2 d\mathbf{x} = 2\beta - \frac{\beta^2}{\pi^2 R^4}\left(\frac{16R^3}{3} + \pi R^2 h\,\big(1+\tan^2\theta\big)\right).$$

We maximize $\mathsf{J}_2(\mathbf{q}_\beta)$ in β to get $\mathsf{J}_2(\mathbf{q}_\beta) = \pi R^2\,/\,\big(\,h/\cos^2\theta\;+\;16R\,/\,3\pi\big)$. ⊠

Remark 4.3. *Bounds* (29) *of Theorem 4.3 seem to be completely new. They have not been previously obtained even heuristically by physical reasoning. This result is especially important in applications related to combustion in turboengines. Indeed, in order to ensure the cooling of the combustion chamber, its wall is perforated by inclined holes. As seen above, the angle of the perforation axis with the plate has a great influence on its Rayleigh conductivity hence on its acoustic properties.*

4.4 Numerical experiments

This section is devoted to a numerical consolidation of the above theoretical bounds obtained for the Rayleigh conductivity in theorems 4.1, 4.2 and 4.3. A numerical approximation $K_{R,*}^{\rm num}$ of the Rayleigh conductivity obtained by a direct numerical simulation of problem (7) is compared with $K_{R,*}^-$ and $K_{R,*}^+$ for $h/R \in [0, 10]$. We have considered two angles $\varphi = 5^o$ and $\varphi = 10^o$ for a conical perforation and $\theta = 15^o$ and $\theta = 30^o$ for an inclined one. The results for straight cylindrical perforations, conical perforations, and inclined perforations are collected in Figures 5, 6 and 7. It is worth mentionning that $K_{R,*}^- \le K_{R,*}^{\rm num} \le K_{R,*}^+$ in all cases.

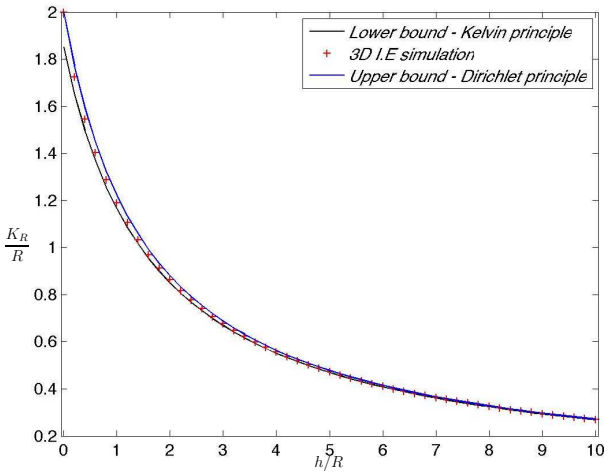

Figure 5: Lower and upper bounds and numerical approximation of the Rayleigh conductivity for a cylindrical perforation

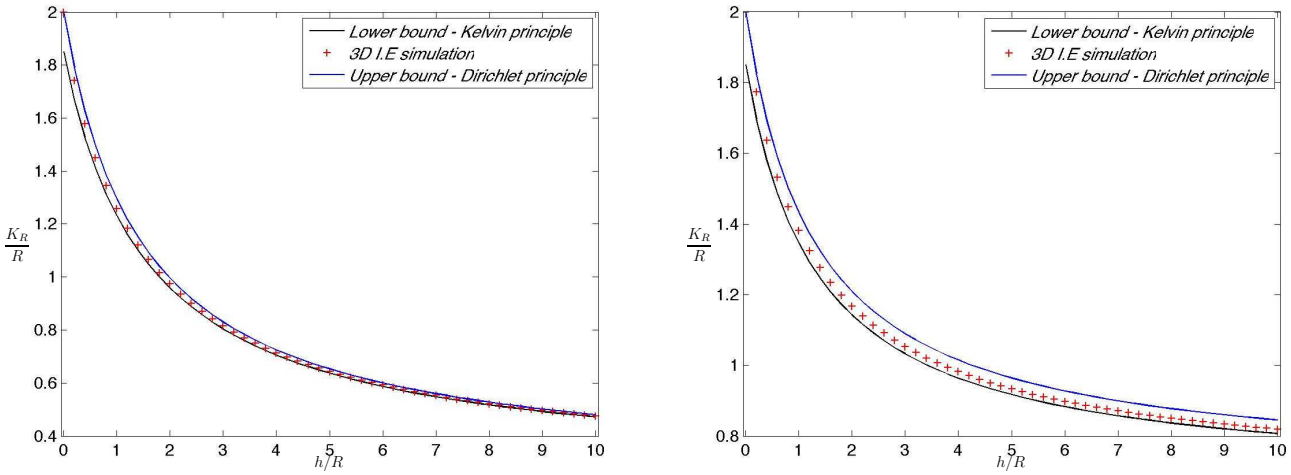

Figure 6: Lower and upper bounds and numerical approximation of the Rayleigh conductivity for a conical perforation with $\varphi = 5^o$ and $\varphi = 15^o$

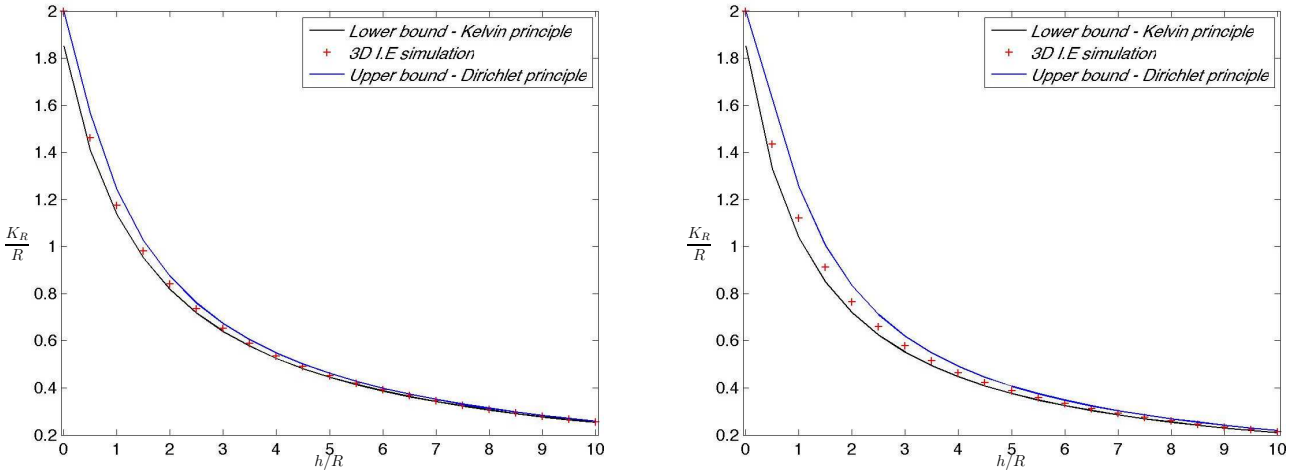

Figure 7: Lower and upper bounds and numerical approximation of the Rayleigh conductivity for an inclined perforation with $\theta = 15^o$ and $\theta = 30^o$

5 Approximate Rayleigh conductivity and corresponding error

5.1 Approximate Rayleigh conductivity

It is quite natural to take the mean value of the above lower and upper bounds for approximating the Rayleigh conductivity:

$$K_R^{\text{app}} = \frac{K_R^+ + K_R^-}{2}. \tag{33}$$

The relative error induced by this approximation is defined as

$$\varepsilon = \left| \frac{K_R - K_R^{\text{app}}}{K_R} \right|.$$

A lower script as $K_{R,\text{inc}}^{\text{app}}$ or ε_{cyl} can be added for mentionning the case being considered.

5.2 Theoretical bound on the error

Since $K_R^- \leq K_R \leq K_R^+$, the error can be bounded as follows:

$$\varepsilon \leq \frac{1}{2}\left(\frac{K_R^+ - K_R^-}{K_R^-}\right). \tag{34}$$

These inequalities are not optimal but give a good idea on the magnitude of the error. The right-hand sides of (34) are depicted in Figure 8 for a conical perforation and in Figure 9 for an inclined perforation. The results for a straight cylindrical perforation are reported in Figure 8 for $\varphi = 0$ or in Figure 9 for $\theta = 0$.

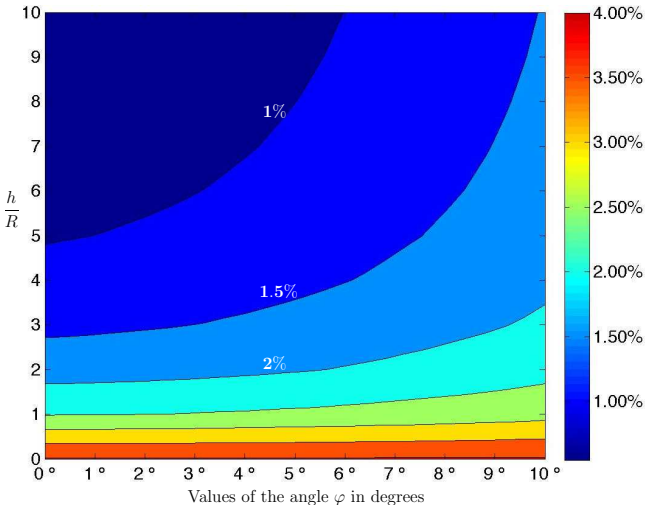

Figure 8: Upper bound of $\varepsilon_{\text{con}} = \left|\frac{K_{R,\text{con}} - K_{R,\text{con}}^{\text{app}}}{K_{R,\text{con}}}\right|$

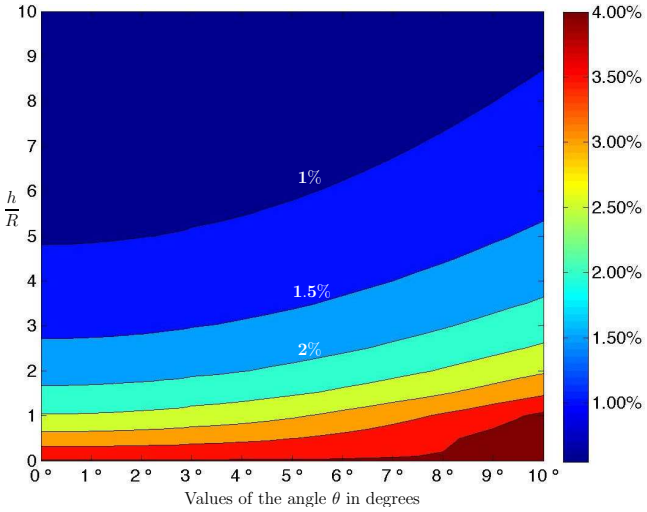

Figure 9: Upper bound of $\varepsilon_{\text{inc}} = \left|\frac{K_{R,\text{inc}} - K_{R,\text{inc}}^{\text{app}}}{K_{R,\text{inc}}}\right|$

Errors for $\varphi \leq 10^o$ and $\theta \leq 10^o$ are less than 5%. For small values of h the error is below 5%. For larger values of h, the bound for the error is lower and mostly less than 2%.

5.3 Numerical study of the error

In this section, we compare a numerical approximation K_R^{num} of the Rayleigh conductivity to its analytical approximation K_R^{app}. For cylindrical and conical perforations, we have considered several configurations each of them corresponding to a set of values for h and φ given in the form of a grid of points with step-sizes $\delta\varphi$ and δh (see Figure 3)

$$\varphi \in [0, 10], \quad h \,/\, R_- \in [0, 10] \quad \text{with steps } \delta\varphi = 0.1 \text{ and } \delta h \,/\, R_- = .2.$$

The values of φ and $\delta\varphi$ are given in degrees. For these axi-symmetric cases, the discret problem to be solved is of small-size. It was hence possible to carry out the computations related to these configurations on a laptop. The geometries for $\varphi = 0$ corresponds to the cylindrical case. The results for a conical perforation are collected in Figure 10.

For inclined perforations, the various configurations are similarly described by means of a grid of points θ and h given by

$$\theta \in [0, 10], \quad h \,/\, R \in [0, 10] \quad \text{with steps } \delta\theta = 0.1 \text{ and } \delta h \,/\, R = .5.$$

Here too, the values of θ and $\delta\theta$ are given in degrees. The geometry is not axi-symmetric. A three dimensional solver was required to perform the computations. To lower the discretization error at a level where it has no significant incidence on the result, we have used very refined meshes. The largest computations involved

$N_{\rm dof} := 1.5\ 10^5$ degrees of freedom requiring to solve square dense linear systems of $N_{\rm dof} \times N_{\rm dof}$ unknowns. The computations were carried out on high performence platform with 400 cores. They took 12 hours of elapsed CPU time. The numerical results for an inclined perforation are collected in Figure 11.

Comparing these figures with Figures 8 and 9, we remark that, for large values of h, inequalities (34) predict too large errors. More precisely, the error is below 1% for $h/R > 1$. This clearly shows that the proposed approximation of the Rayleigh conductivity can advantageously replace the direct computation.

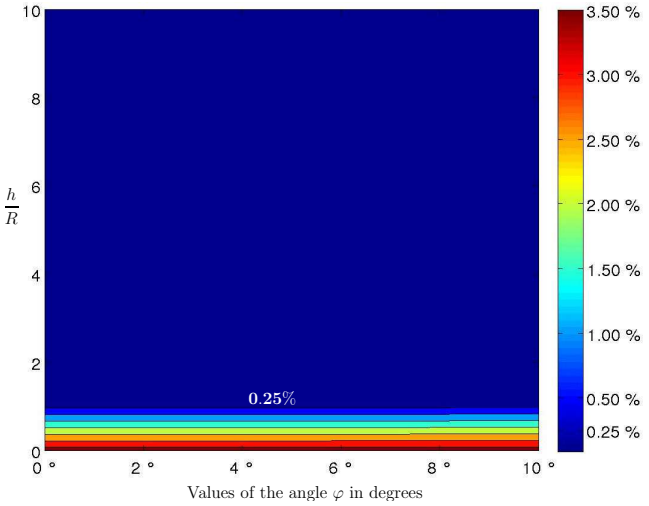

Figure 10: The error $\varepsilon_{\rm con} = \left| \frac{K^{\rm app}_{R,{\rm con}} - K^{\rm num}_{R,{\rm con}}}{K^{\rm num}_{R,{\rm con}}} \right|$

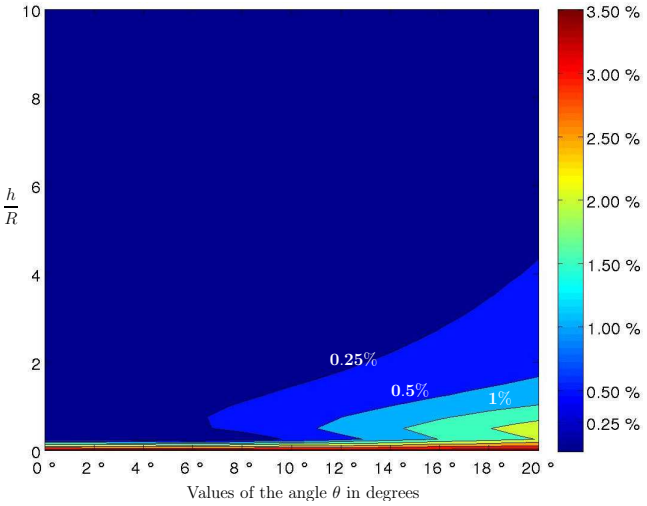

Figure 11: The error $\varepsilon_{\rm inc} = \left| \frac{K^{\rm app}_{R,{\rm inc}} - K^{\rm num}_{R,{\rm inc}}}{K^{\rm num}_{R,{\rm inc}}} \right|$

In Figures 12 and 13 we compute the barycentric coefficients $\lambda_* \in [0,1]$ of $K_{R,*}$ with respect to $K^{\pm}_{R,*}$

$$K_{R,{\rm con}} \ = \ (1-\lambda_{\rm con})\, K^-_{R,{\rm con}} \ + \ \lambda_{\rm con}\, K^+_{R,{\rm con}} \quad \text{and} \quad K_{R,{\rm inc}} \ = \ (1-\lambda_{\rm inc})\, K^-_{R,{\rm inc}} \ + \ \lambda_{\rm inc}\, K^+_{R,{\rm inc}}.$$

The best approximation of K_R is K^-_R for $\lambda \in [0, 1/4]$, $K^{\rm app}_R$ for $\lambda \in [1/4, 3/4]$, and K^+_R for $\lambda \in [3/4, 1]$. It can be observed that for small ratio of h/R, the best approximation of K_R is given by K^+_R, whereas for larger h/R, it is given by $K^{\rm app}_R$. These maps also indicate that the approximation defined in (33) is very accurate in most configurations.

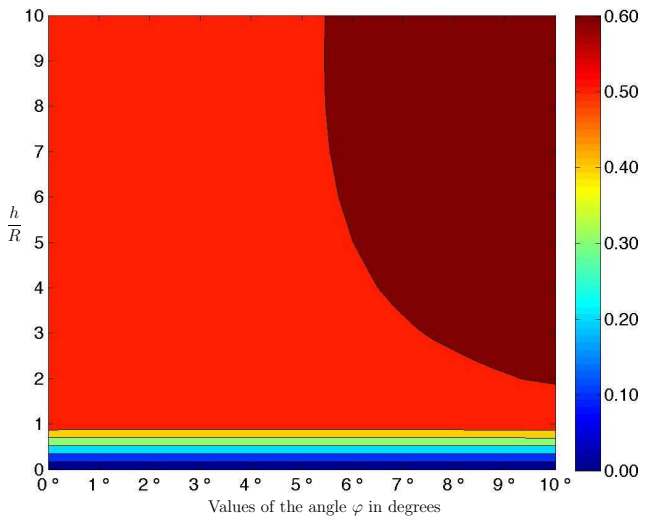

Figure 12: The barycentric coordinate λ_{con}

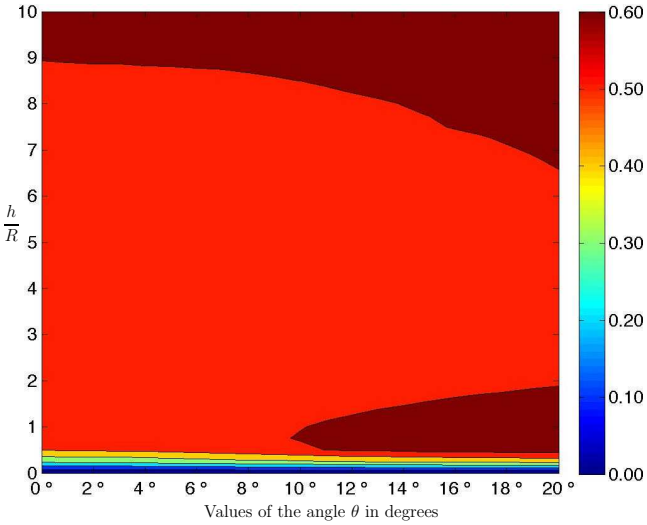

Figure 13: The barycentric coordinate λ_{cyl}

Acknowledgements

This work was supported by the French National Research Agency under grant no. ANR−08−SYSC−001. We would like to thank the CEA-CCRT (Centre de calcul pour la recherche et la technologie) for providing us with the possibility of using the Titane computer.

A Appendix: calculation of some integrals

Let us recall that w_R, t_R, z_R are defined in (21), (30) and (25), are given by

$$f_R(\mathbf{x}) = \frac{1}{2\pi}\int_{\mathsf{B}_R} \rho_{f_R}(\mathbf{y})\frac{ds_{\mathbf{y}}}{|\mathbf{x}-\mathbf{y}|} \quad \text{for } x_3 \neq 0,$$

with $f_R = w_R$, t_R or z_R and the single layer potential ρ_{f_R} defined on $\mathsf{B}_R = \{(y_1, y_2, y_3) \in \mathbb{R}^3 \mid y_1^2 + y_2^2 < R^2 \text{ and } y_3 = 0\}$ by

$$\rho_{w_R}(\mathbf{x}) = \frac{1}{\pi}\frac{1}{\sqrt{R^2-|\mathbf{y}|^2}}, \quad \rho_{t_R}(\mathbf{x}) = \frac{4}{\pi}\frac{y_1}{\sqrt{R^2-|\mathbf{y}|^2}}, \quad \text{and} \quad \rho_{z_R}(\mathbf{x}) = 1.$$

The following lemma collects three of the integrals involved in the bounds of the Rayleigh conductivity.

Lemma A.1. *The following formulas hold true*

$$\begin{aligned}
&\textit{(i)} && \int_{x_3>0} \left|\nabla w_R(\mathbf{x})\right|^2 d\mathbf{x} &&= \int_{x_3<0} \left|\nabla w_R(\mathbf{x})\right|^2 d\mathbf{x} &&= R,\\
&\textit{(ii)} && \int_{x_3>0} \left|\nabla t_R(\mathbf{x})\right|^2 d\mathbf{x} &&= \int_{x_3<0} \left|\nabla t_R(\mathbf{x})\right|^2 d\mathbf{x} &&= 8R^3/3,\\
&\textit{(iii)} && \int_{x_3>0} \left|\nabla z_R(\mathbf{x})\right|^2 d\mathbf{x} &&= \int_{x_3<0} \left|\nabla z_R(\mathbf{x})\right|^2 d\mathbf{x} &&= 8R^3/3.
\end{aligned}$$

Proof. Due to symmetry, we have for $f_R = w_R$, z_R or t_R

$$I_{f_R} = \int_{x_3<0} \left|\nabla f_R(\mathbf{x})\right|^2 d\mathbf{x} = \int_{x_3>0} \left|\nabla f_R(\mathbf{x})\right|^2 d\mathbf{x}.$$

Since $f_R \in \mathsf{BL}(\{x_3 > 0\})$ and $\Delta f_R = 0$, we get, from Green's formula and the integral representations of the solution to the related boundary value problems [23]

$$I_{f_R} = \int_{x_3>0} \left|\nabla f_R(\mathbf{x})\right|^2 d\mathbf{x} = \int_{x_3=0} \partial_{x_3} f_R(\mathbf{x}) f_R(\mathbf{x}) ds_{\mathbf{x}} = \int_{\mathsf{B}_R} \rho_{f_R}(\mathbf{x}) f_R(\mathbf{x}) ds_{\mathbf{x}}. \tag{35}$$

(i) From (21), we set $w_R = 1/2$ on B_R. This leads to

$$I_{w_R} = \int_{\mathsf{B}_R} \frac{1}{\pi\sqrt{R^2 - |\mathbf{y}|^2}} \frac{1}{2} ds_{\mathbf{y}} = \int_0^R \frac{\rho d\rho}{\sqrt{R^2 - \rho^2}} = \left[\sqrt{R^2 - \rho^2}\right]_0^R = R.$$

(ii) Similarly, from (30), we have $t_R(\mathbf{x}) = x_1$ on B_R. In spherical coordinates, integral (35) takes the form, with $y_1 = \rho\, \cos(\widehat{\theta})$, $y_2 = \rho\, \sin(\widehat{\theta})\, \cos(\widehat{\varphi})$, and $y_3 = \rho\, \sin(\widehat{\theta})\, \sin(\widehat{\varphi})$,

$$I_{t_R} = \int_{\mathsf{B}_R} \frac{4}{\pi} \frac{y_1}{\sqrt{R^2 - |\mathbf{y}|^2}}\, y_1 ds_{\mathbf{y}} = \frac{4}{\pi} \int_0^R \int_0^{2\pi} \frac{\rho\, \cos(\widehat{\theta})}{\sqrt{R^2 - \rho^2}}\, \rho\, \cos(\widehat{\theta})\, \rho\, d\rho d\widehat{\theta} \tag{36}$$

$$= \frac{4}{\pi} \int_0^R \frac{\rho^3}{\sqrt{R^2 - \rho^2}}\, d\rho \int_0^{2\pi} \cos^2(\widehat{\theta}) d\widehat{\theta} = -4 \left[\frac{\rho^2 - 2R^2}{3} \sqrt{R^2 - \rho^2}\right]_{\rho=0}^R = \frac{8R^3}{3}. \tag{37}$$

(iii) In this case, we do not know explicitly the value of z_R on B_R. However, I_{z_R} is given by

$$I_{z_R} = \frac{1}{2\pi} \int_{\mathsf{B}_R} \int_{\mathsf{B}_R} \frac{ds_{\mathbf{y}} ds_{\mathbf{x}}}{|\mathbf{y} - \mathbf{x}|} \;=\; \frac{R^3}{2\pi} \int_{B_1} \int_{B_1} \frac{ds_{\mathbf{y}} ds_{\mathbf{x}}}{|\mathbf{y} - \mathbf{x}|}.$$

To evaluate this integral, we use Copson's formula [3]

$$\int_{B_1} \frac{ds_{\mathbf{y}}}{|\mathbf{x} - \mathbf{y}|} \;=\; 4 \int_{\rho=0}^1 \int_{t=0}^{\mathbf{min}(\rho,r)} \frac{\rho\, d\rho\, dt}{\sqrt{(\rho^2 - t^2)(r^2 - t^2)}}.$$

Separating the cases $r < \rho$ and $\rho < r$, this leads to

$$\begin{aligned} I_{z_R} &= \frac{2R^3}{\pi} \int_{B_1} \left(\int_{\rho=0}^1 \int_{t=0}^{\mathbf{min}(\rho,r)} \frac{\rho\, d\rho\, dt}{\sqrt{(\rho^2 - t^2)(r^2 - t^2)}} \right) ds_{\mathbf{x}} \\ &= 4R^3 \int_{r=0}^1 \int_{\rho=0}^1 \int_0^{\mathbf{min}(\rho,r)} \frac{r\rho dr d\rho dt}{\sqrt{(\rho^2 - t^2)(r^2 - t^2)}} \\ &= 4R^3 \int_{r=0}^1 \int_{\rho=r}^1 \int_{t=0}^r \frac{r\rho dr d\rho dt}{\sqrt{(\rho^2 - t^2)(r^2 - t^2)}} + 4R^3 \int_{r=0}^1 \int_{\rho=0}^r \int_{t=0}^\rho \frac{r\rho dr d\rho dt}{\sqrt{(\rho^2 - t^2)(r^2 - t^2)}}. \end{aligned} \tag{38}$$

Taking into account symmetry and commuting the integrals, we get

$$I_{z_R} = 8R^3 \int_{r=0}^1 \int_{\rho=0}^1 \int_{t=0}^\rho \frac{r\rho dr d\rho dt}{\sqrt{(\rho^2 - t^2)(r^2 - t^2)}} = 8R^3 \int_{t=0}^1 \int_{\rho=t}^r \int_{r=\rho}^1 \frac{r\rho dr d\rho dt}{\sqrt{(\rho^2 - t^2)(r^2 - t^2)}}.$$

Evaluating successively the integrals, we get

$$\begin{aligned} I_{z_R} &= 8R^3 \int_{t=0}^1 \int_{\rho=t}^1 \left[\frac{\sqrt{r^2 - t^2}}{\sqrt{\rho^2 - t^2}}\right]_{r=\rho}^1 \rho d\rho dt \;=\; 8R^3 \int_{t=0}^1 \int_{\rho=t}^r \left(\frac{\sqrt{1 - t^2}}{\sqrt{\rho^2 - t^2}} - 1\right) \rho d\rho dt, \\ &= 8R^3 \int_{t=0}^1 \left[\sqrt{1 - t^2}\sqrt{\rho^2 - t^2} - \frac{\rho^2}{2}\right]_{\rho=t}^1 dt \;=\; 8R^3 \int_{t=0}^1 \left(\frac{1}{2} - \frac{t^2}{2}\right) dt \;=\; \frac{8R^3}{3}. \qquad \boxtimes \end{aligned}$$

References

[1] M. Alster. Improved calculation of resonant frequencies of Helmholtz resonators. *Journal of Sound and Vibration*, 24(1):63–85, 1972.

[2] R. C. Chanaud. Effects of geometry on the resonance frequency of Helmholtz resonators, part II. *Journal of sound and vibration*, 204(5):829–834, 1997.

[3] E.T. Copson. On the problem of the electrified disc. *Proceedings of the Edinburgh Mathematical Society (Series 2)*, 8(01):14–19, 1947.

[4] R. Courant and D. Hilbert. *Methods of mathematical physics. Vol. I.* Interscience Publishers, Inc., New York, N.Y., 1953.

[5] B. Enquist and A. Majda. Absorbing boundary conditions for the numerical simulation of wave. *Mathematics of Computation*, 31:629–651, 1977.

[6] J. Giroire. *Etude de quelques problèmes aux limites extérieurs et résolution par équations intégrales.* PhD thesis, Paris VI, 1987.

[7] M.S. Howe. On the theory of unsteady high Reynolds number flow through a circular aperture. *Proceedings of the Royal Society of London. A. Mathematical and Physical Sciences*, 366(1725):205, 1979.

[8] M.S. Howe. Influence of wall thickness on Rayleigh conductivity and flow-induced aperture tones. *Journal of fluids and structures*, 11(4):351–366, 1997.

[9] M.S. Howe. *Acoustics of fluid-structure interactions.* Cambridge Univ. Press, 1998.

[10] U. Ingard. On the theory and design of acoustic resonators. *The Journal of the acoustical society of America*, 25:1037–1061, 1953.

[11] J.B. Keller and D. Givoli. Exact non-reflecting boundary conditions. *Journal of Computational Physics*, 82(1):172–192, 1989.

[12] E. Kerschen, A. Cain, and G. Raman. Analytical modeling of Helmholtz resonator based powered resonance tubes. In *2nd AIAA Flow Control Conference*, 2004.

[13] D.G. Luenberger. *Optimization by vector space methods.* Wiley-Interscience, 1997.

[14] C. Macaskill and E.O. Tuck. Evaluation of the acoustic impedance of a screen. *The Journal of the Australian Mathematical Society. Series B. Applied Mathematics*, 20(01):46–61, 1977.

[15] C. Malmary. *Etude théorique et expérimentale de l'impédance acoustique de matériaux en présence d'un écoulement d'air tangentiel.* PhD thesis, Univ. du Maine, 2000.

[16] T.H. Melling. The acoustic impendance of perforates at medium and high sound pressure levels. *Journal of Sound and Vibration*, 29(1):1–65, 1973.

[17] S. Mendez and JD Eldredge. Acoustic modeling of perforated plates with bias flow for Large-Eddy Simulations. *Journal of Computational Physics*, 228(13):4757–4772, 2009.

[18] J. Mohring. Helmholtz resonators with large aperture. *Acta Acoustica united with Acoustica*, 85(6):751–763, 1999.

[19] C.L. Morfey. Acoustic properties of openings at low frequencies. *Journal of Sound and Vibration*, 9(3):357–366, 1969.

[20] R.L. Panton and J.M. Miller. Resonant frequencies of cylindrical Helmholtz resonators. *The Journal of the Acoustical Society of America*, 57:1533–1535, 1975.

[21] J.W.S. Rayleigh. *The Theory of Sound, vols. 1 and 2.* Dover Publications, New York, 1945.

[22] J.E. Roberts and J.-M. Thomas. Mixed and hybrid methods. In *Handbook of numerical analysis. Vol. 2.* Elsevier Science Publishers, 1991.

[23] S. Sauter and C. Schwab. *Boundary Element Methods, vol. 39 of Springer Series in Computational Mathematics.* Springer, Heidelberg, 2010.

[24] I.N. Sneddon. *Mixed boundary value problems in potential theory.* North-Holland Pub. Co., 1966.

[25] E.O. Tuck. Matching problems involving flow through small holes. *Advances in applied mechanics*, 15:89–158, 1975.